

Coupled Modulational Instability of Copropagating Spin Waves in Magnetic Thin Films

Mingzhong Wu¹ and Boris A. Kalinikos²

¹*Department of Physics, Colorado State University, Fort Collins, Colorado 80523, USA*

²*St. Petersburg Electrotechnical University, 197376, St. Petersburg, Russia*

(Received 23 April 2008; published 11 July 2008)

This Letter reports the first results on the coupled modulational instability of copropagating spin waves in a magnetic film. Strong instability was observed for the two waves with either attractive or repulsive nonlinearity. If the two waves have attractive nonlinearity, the instability leads to the formation of bright solitons. If the two waves have repulsive nonlinearity, the process results in the formation of black solitons. The instability was also observed for the two waves in separated attractive-repulsive nonlinearity regimes.

DOI: [10.1103/PhysRevLett.101.027206](https://doi.org/10.1103/PhysRevLett.101.027206)

PACS numbers: 85.70.Ge, 05.45.Yv, 75.30.Ds, 76.50.+g

Modulational instability refers to a nonlinear process in which a weak modulation on the envelope of a continuous wave can grow exponentially. Modulational instability has been observed in many nonlinear dispersive systems [1–10]. It can lead to many interesting phenomena, including soliton formation [2,5], chaotic excitation [3], and Fermi-Pasta-Ulam recurrence [6,7].

Modulational instability is called spontaneous modulational instability (SMI) if the initial modulation is developed from the noise in the system. Two copropagating waves with *comparable* group velocity and dispersion properties can give rise to an amplitude-modulated wave. Modulational instability developed from such a modulated wave is called induced modulational instability (IMI). In spite of being initiated differently, the SMI and IMI processes are both realized through four-wave nonlinear interactions [1].

The SMI and IMI responses are generally described by the nonlinear Schrödinger equation (NLSE) [1,11]. In the context of the NLSE analysis, the SMI and IMI scenarios occur only for the waves with attractive nonlinearity. In practice, however, the processes were observed in both the attractive [1,2] and the repulsive [5,9] nonlinearity regimes. Note that the key factors that determine the nature of nonlinearity are the dispersion coefficient D and the nonlinearity coefficient N . Physically, these two parameters represent the curvature of the frequency versus wave number dispersion and the change in frequency with wave amplitude, respectively. If $DN < 0$, one has attractive nonlinearity; if $DN > 0$, one has repulsive nonlinearity [12].

For two copropagating waves, it is more general that the waves have significantly *different* frequencies, group velocity, or dispersion properties. In this situation, the four-wave interaction cannot be phase matched and thereby will not occur, and the usual NLSE analysis also does not apply. Can such waves exhibit modulational instability? This question has stimulated considerable theoretical work [13–19]. In particular, the work by Agrawal [13] and McKinstrie and Luther [16] showed two things. (1) The two waves with attractive nonlinearity can interact to pro-

duce a *coupled modulational instability* (CMI), of which the growth rate is larger than that of either wave alone. (2) The CMI effect also exists for the two waves in the repulsive nonlinearity regime. This work was based on the model of two nonlinear Schrödinger equations coupled through cross-phase modulation. With the method of Zakharov, Yu, McKinstrie, and Agrawal conducted similar analyses but obtained *contrary* results [18]. (1) The two waves with attractive nonlinearity are modulationally unstable by themselves but do not cooperate to produce a CMI response unless their group velocities are comparable. (2) The two waves with repulsive nonlinearity are modulationally stable. They also found that the CMI process occurs for the two waves which are in the separate attractive-repulsive nonlinearity regimes but have comparable group velocities [18]. In spite of these contrary predictions, there has been no experimental work on the subject.

This Letter reports the first experimental results on coupled modulational instability. The experiments used dipole-exchange spin waves in a magnetic yttrium iron garnet (YIG) thin film. Strong CMI effects were observed for two copropagating spin waves with either attractive or repulsive nonlinearity. When both waves are in the attractive regime, the CMI process leads to the formation of bright solitons. When both waves are in the repulsive regime, the process leads to the formation of black solitons. The CMI response was also observed for the two waves in separate attractive-repulsive regimes. These results manifest themselves even for the two waves with significantly different group velocity and dispersion properties.

Figure 1 shows the experimental setup. The YIG film is magnetized to saturation by a static magnetic field perpendicular to the film plane. This configuration allows for the propagation of forward volume spin waves with a positive nonlinearity coefficient [20,21]. Two microstrip transducers with a separation of about 10 mm are placed over the YIG strip for the excitation and detection of spin waves. The detected signals are analyzed with a broadband oscilloscope and a power spectrum analyzer. For the data

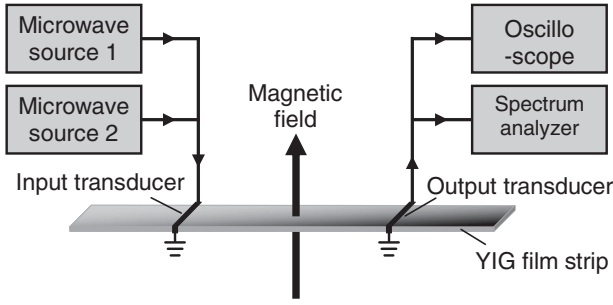


FIG. 1. Diagram of experimental setup.

shown in Figs. 2–4, the YIG strip was $6.8 \mu\text{m}$ in thickness, 2.2 mm in width, and 46.0 mm in length, and the magnetic field was 3189 Oe . For the data in Figs. 5 and 6, the YIG strip was $5.2 \mu\text{m}$ in thickness, 1.9 mm in width, and 22.5 mm in length, and the field was 2776 Oe .

The YIG films had pinned surface spins and, therefore, supported the propagation of dipole-exchange spin waves (DESWs) [22]. Figure 2 shows the DESW properties for the $6.8 \mu\text{m}$ -thick YIG film strip. Figure 2(a) shows the calculated wave number (k) versus frequency (ω) dispersion curves. The calculation was done with the DESW theory [22] and for the parameters given above. Other parameters include a saturation induction of 1750 G , an exchange constant of $3.2 \times 10^{-12} \text{ cm}^2$, and an anisotropy field of 31 Oe . Figure 2(b) shows the measured transmission loss characteristic of the YIG strip-transducer structure shown in Fig. 1. The measurement was done in a linear regime with an input power of 1 mW . Figures 2(c) and 2(d) show the dispersion curves in Fig. 2(a) and the transmission curve in Fig. 2(b), respectively, in expanded frequency scales.

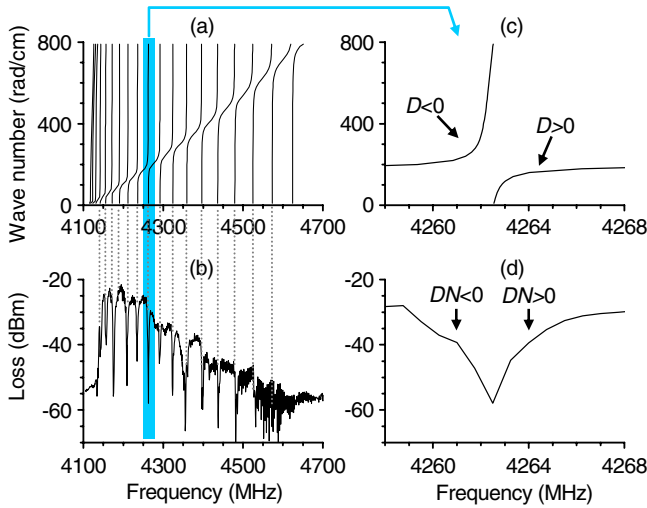


FIG. 2 (color online). Characteristics of dipole-exchange spin waves. (a) Calculated wave number vs frequency dispersion curves. (b) Measured transmission loss vs frequency curve for a YIG strip-transducer structure. (c) Part of the dispersion curves shown in (a). (d) Part of the transmission curve shown in (b).

As shown in Fig. 2(a), there are gaps between neighboring DESW dispersion curves. These gaps are called “dipole gaps.” At each gap frequency, the group velocity $v_g = \partial\omega/\partial k$ is close to zero. This results in high transmission loss at the gap frequencies and thereby the existence of dips at the same frequencies in the measured transmission loss versus frequency curves, as shown in Fig. 2(b). In other words, the dips in the transmission curves indicate dipole gap frequencies. The data in Figs. 2(a) and 2(b) show good agreement between the calculated gap frequencies and the frequencies of the transmission dips, as indicated by vertical dotted lines.

Figure 2(c) shows the dispersion curves for the dipole gap at 4262.5 MHz . Figure 2(d) shows the corresponding transmission dip. Two important points about the DESW properties are evident in Fig. 2(c). First, the slope of the dispersion curves changes significantly with frequency. This means that the group velocity has a strong dependence on frequency. Second, the signs of curvatures of the two dispersion curves are opposite. This means that, through a change in frequency, one can easily achieve different types of nonlinearity, as indicated in Fig. 2(d). Note that the nonlinearity coefficient N is positive, as mentioned above. These properties played a key role in the CMI effects reported below.

Figure 3 shows the data for two copropagating waves both with attractive nonlinearity. The waves were excited by two input microwave signals. The input frequencies were $f_1 = 4263.2 \text{ MHz}$ and $f_2 = 4263.3 \text{ MHz}$. The input powers were $P_1 = 2 \text{ mW}$ and $P_2 = 40 \text{ mW}$. Figure 3(a) shows a transmission dip and the locations of the input frequencies relative to the dip frequency. The transmission curve was measured at an input power of 63 mW . The dashed lines indicate the input frequencies. Figures 3(b)–3(d) show the power-frequency spectrum, power-time profile, and phase-time profile, respectively, for the output signals.

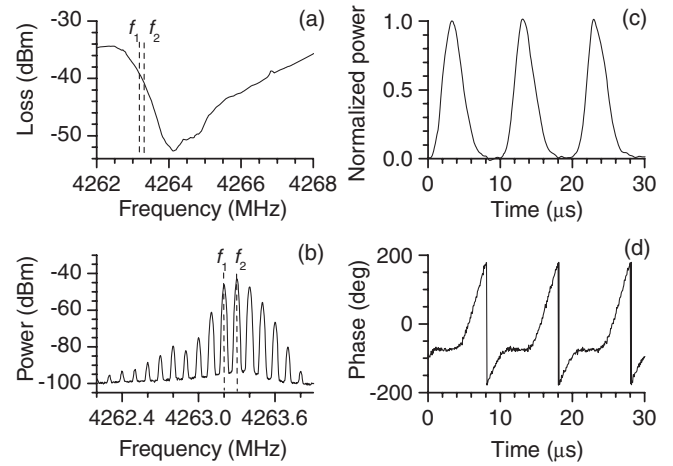


FIG. 3. Coupled modulational instability of two waves with attractive nonlinearity. Graph (a) shows a transmission curve and the locations of the input frequencies. Graphs (b), (c), and (d) show the power spectrum, power-time profile, and phase-time profile, respectively, for the output signals.

file, and phase-time profile, respectively, for the output signals. In Fig. 3(b), the two peaks corresponding to the input frequencies are labeled with f_1 and f_2 . The power in Fig. 3(c) is shown in a normalized scale. The phase change in Fig. 3(d) was measured relative to a reference wave of frequency f_2 [23].

Figure 3(a) indicates that both of the two input frequencies were positioned in the $DN < 0$ region, namely, an attractive nonlinearity regime. Note that the transmission dip in Fig. 3(a) occurs at a frequency slightly higher than that in Fig. 2(d) due to a nonlinear frequency shift. Figure 3(b) shows a rich frequency comb. The frequencies of the two main peaks are exactly the same as the input frequencies. The other peaks result from the new DESW modes that were excited through the CMI process. In the time domain, the CMI process led to the formation of a train of bright envelope solitons, as shown in Fig. 3(c). The phase profile in Fig. 3(d) is flat across the central portion of each soliton. Such a flat phase profile is a key signature for bright solitons [23].

Now we turn to the case where both waves have repulsive nonlinearity. Figure 4 shows the representative data. The format is the same as for Fig. 3. The input frequencies were $f_1 = 4265.5$ MHz and $f_2 = 4265.55$ MHz. The input powers were $P_1 = 10$ mW and $P_2 = 25$ mW. The transmission curve in Fig. 4(a) is exactly the same as that in Fig. 3(a).

Figure 4(a) indicates that the two input frequencies are in the repulsive nonlinearity regime. Figure 4(b) shows a rich frequency comb. As in Fig. 3(b), the two main peaks exactly match the two input frequencies, and the other peaks indicate the CMI-excited new modes. In the time domain, the waveform and phase profile are in a stark contrast to those shown in Fig. 3. One observes a train of black envelope solitons, as in Fig. 4(c), and 180° phase

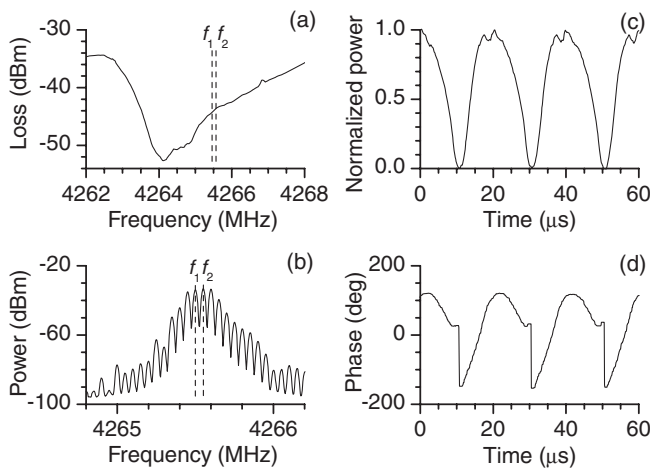


FIG. 4. Coupled modulational instability of two waves with repulsive nonlinearity. Graph (a) shows a transmission curve and the locations of the input frequencies. Graphs (b), (c), and (d) show the power spectrum, power-time profile, and phase-time profile, respectively, for the output signals.

jumps across each soliton dip, as in Fig. 4(d). This phase jump is a signature for black solitons [5].

The data in Figs. 3 and 4 show the key results, namely, that the CMI effect is realized for the two waves with attractive or repulsive nonlinearity. These results agree with the predictions by Agrawal [13] and McKinstrie and Luther [16] but differ from the analyses by Yu, McKinstrie, and Agrawal [18]. The data also demonstrate that the CMI process can lead to the formation of bright solitons for the waves with attractive nonlinearity and black solitons for the waves with repulsive nonlinearity. This response is the same as for SMI and IMI processes [2,5,9]. It is also important to note that both the frequency combs have uniform separations. This means that the modulation frequencies are equal to the difference between the two input frequencies, as predicted by Agrawal [13,14].

The data also show that the occurrence of the CMI response does not require the group velocities of the two waves to be comparable. Figure 5 shows representative data obtained for the two waves with attractive nonlinearity. In each graph, the left part shows the power-time profile of the output signal, and the right part gives the frequencies and the calculated group velocities and dispersion coefficients of the two waves. The nominal input powers were $P_1 = 32$ mW and $P_2 = 126$ mW. Note that the difference in group velocity is relatively small in Fig. 5(a) and is relatively large in Fig. 5(c).

Figure 5 shows that the copropagating waves cooperate to produce strong CMI responses no matter whether the group velocities are comparable or significantly different. This result agrees with Agrawal's analyses [13] but is contrary to the predictions by Yu, McKinstrie, and Agrawal [18]. Recall that the work by Yu, McKinstrie, and Agrawal indicated that the CMI effect of the two waves

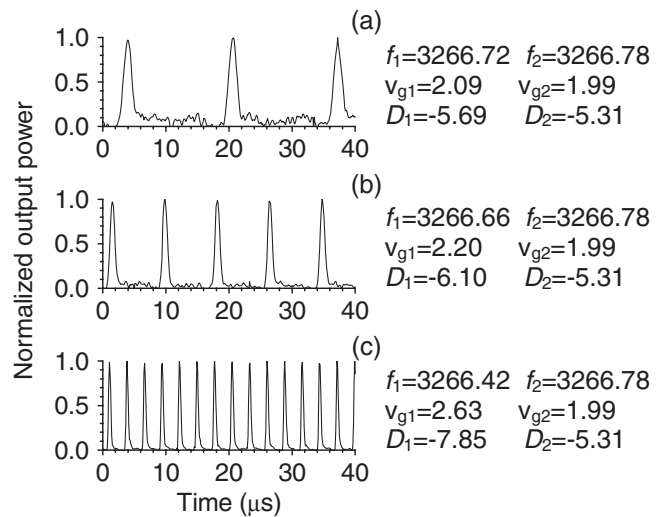


FIG. 5. Time-domain output signals for two initial waves with attractive nonlinearity. In each graph, the right side gives the frequencies (MHz), group velocities (10^5 cm/s), and dispersion coefficients (10^3 cm²/s) of the initial waves.

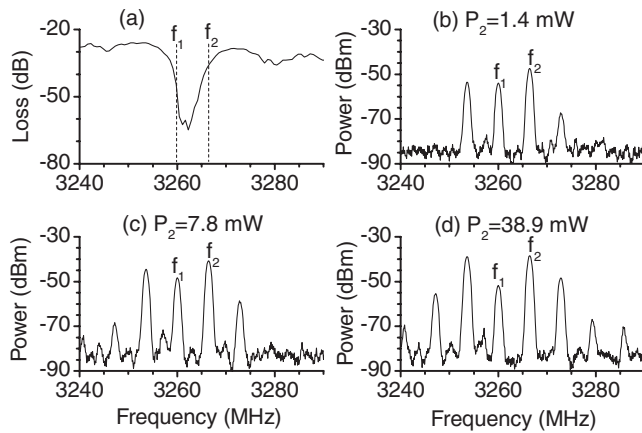


FIG. 6. Coupled modulational instability of two waves with different types of nonlinearity. Graph (a) shows a transmission curve and the locations of the input frequencies. Graphs (b)–(d) show the power spectrum for the output signals for different input power P_2 , as indicated. The input power P_1 is constant.

with attractive nonlinearity would not occur unless the group velocity difference between the two waves were made very small.

The results presented above are for the two waves in the same nonlinearity regime. Turn now to the two waves in separate attractive-repulsive nonlinearity regimes. Figure 6 show representative data. Figure 6(a) shows a transmission loss curve measured at an input power of 1 mW and the location of the input frequencies. Figures 6(b)–6(d) show the power spectrum for output signals for different input power P_2 . The input power P_1 is 27.5 mW. Figure 6(a) indicates that the two waves have different types of nonlinearity. Figures 6(b)–6(d) indicate that the two waves interact to produce new modes. Also, the higher the input power, the more the new modes. These results mean that the CMI process also occurs for the two waves with different types of nonlinearity. This is in agreement with the prediction by Yu, McKinstrie, and Agrawal [18].

Note that the CMI effect had been observed for a wide range of power levels (1–150 mW) and frequencies, and the data reported above are only representative examples. The higher the power level is, the stronger the CMI effect is. When the frequencies of the initial waves are close to the dipole gap frequencies, higher power is needed for the onset of CMI. The generation of solitons, however, happens only in relatively narrow power and frequency ranges. For the measurements on the two waves with attractive nonlinearity, for example, well-defined bright solitons were observed only for the difference between the input frequencies less than 1 MHz.

It is important to emphasize that the CMI effect reported above differs from the IMI effect of two spin waves reported in Refs. [2,5]. The previous work was done with weakly dispersive magnetostatic waves. For this reason, the initial two waves had very similar group velocity and

dispersion properties, and the modulational instability was realized through a four-wave process and could be well described by the standard NLSE model. In stark contrast, the work reported above was done with strongly dispersive dipole-exchange spin waves. As a result, the two initial waves can have significantly different group velocities and dispersion coefficients, and the standard NLSE model does not apply.

This work was supported in part by the U.S. Army Research Office (No. W911NF-04-1-0247), the U.S. National Science Foundation (No. ECCS-0725386), and the Russian Foundation for Basic Research (No. 08-02-00959).

- [1] M. Remoissenet, *Waves Called Solitons: Concepts and Experiments* (Springer, Berlin, 1995).
- [2] V. E. Demidov, JETP Lett. **68**, 869 (1998).
- [3] M. J. Ablowitz, J. Hammack, D. Henderson, and C. M. Schober, Phys. Rev. Lett. **84**, 887 (2000).
- [4] D. Kip, M. Soljacic, M. Segev, E. Eugenieva, and D. N. Christodoulides, Science **290**, 495 (2000).
- [5] H. Benner, B. A. Kalinikos, N. G. Kovshikov, and M. P. Kostylev, JETP Lett. **72**, 213 (2000).
- [6] G. Van Simaey, Ph. Emplit, and M. Haelterman, Phys. Rev. Lett. **87**, 033902 (2001).
- [7] N. N. Akhmediev, Nature (London) **413**, 267 (2001).
- [8] Z. Chen, S. M. Sears, H. Martin, D. N. Christodoulides, and M. Segev, Proc. Natl. Acad. Sci. U.S.A. **99**, 5223 (2002).
- [9] M. Wu, B. A. Kalinikos, and C. E. Patton, Phys. Rev. Lett. **93**, 157207 (2004).
- [10] H. Segur and D. M. Henderson, Eur. J. Phys. Special Topics **147**, 25 (2007).
- [11] A. Hasegawa, Opt. Lett. **9**, 288 (1984).
- [12] C. Sulem and P. L. Sulem, *The Nonlinear Schrödinger Equation: Self-Focusing and Wave Collapse* (Springer-Verlag, New York, 1999).
- [13] G. P. Agrawal, Phys. Rev. Lett. **59**, 880 (1987).
- [14] J. E. Rothenberg, Phys. Rev. Lett. **64**, 813 (1990).
- [15] G. P. Agrawal, Phys. Rev. Lett. **64**, 814 (1990).
- [16] C. J. McKinstrie and G. G. Luther, Phys. Scr. **T30**, 31 (1990).
- [17] S. V. Vladimirov and V. N. Tsytovich, Phys. Lett. A **171**, 360 (1992).
- [18] M. Yu, C. J. McKinstrie, and G. P. Agrawal, Phys. Rev. E **48**, 2178 (1993).
- [19] E. V. Doktorov and M. A. Molchan, Phys. Scr. **76**, 558 (2007).
- [20] D. D. Stancil, *Theory of Magnetostatic Waves* (Springer-Verlag, New York, 1993).
- [21] P. Kabos and V. S. Stalmachov, *Magnetostatic Waves and Their Applications* (Chapman and Hall, London, 1994).
- [22] B. A. Kalinikos, in *Linear and Nonlinear Spin Waves in Magnetic Films and Superlattices*, edited by M. G. Cottam (World Scientific, Singapore, 1994), Chap. 2.
- [23] J. M. Nash, P. Kabos, R. Staudinger, and C. E. Patton, J. Appl. Phys. **83**, 2689 (1998).